

**Calculation of density and heat capacity of silicon  
by molecular dynamics simulation**

R Kojima Endo, Y Fujihara, M Susa

Department of Metallurgy and Ceramics Science, Tokyo Institute of  
Technology,  
Ookayama, Meguro-ku, Tokyo, 152-8552, Japan;

E-mail: rie@mtl.titech.ac.jp

**Abstract**

The density and molar heat capacity at constant pressure of silicon have been determined with use of molecular dynamics (MD) simulation. The interaction between silicon atoms was expressed by the Stillinger-Weber potential and MD calculation was conducted on crystalline, liquid and amorphous states of silicon at temperatures between 100 and 3000 K. The density and heat capacity obtained are shown as follows:

Density ( $\rho$ ) in  $\text{gcm}^{-3}$ :

Crystalline silicon       $\rho = 2.33 - 2.19 \times 10^{-5}T$       (100 - 1700 K)

Liquid silicon  $\rho = 2.54 - 2.19 \times 10^{-5}T - 1.21 \times 10^{-8}T^2$  (1700 – 3000 K)

Amorphous silicon  $\rho = 2.44 - 5.44 \times 10^{-5}T$  (200 – 1000 K)

Molar heat capacity at constant pressure ( $C_p$ ) in  $\text{Jmol}^{-1}\text{K}^{-1}$ :

Crystalline silicon  $C_p = 23.5 + 3.05 \times 10^{-3}T - 2.93 \times 10^{-7}T^2$  (300 - 1700 K)

Liquid silicon  $C_p = 29.0$  (1700 – 2500 K)

Amorphous silicon  $C_p = 13.1 + 2.25 \times 10^{-2}T - 8.30 \times 10^{-6}T^2$  (300 – 1000 K)

It has been found that the density of amorphous silicon is greater than that of crystalline silicon at temperatures below 1000 K and that the heat capacity of amorphous silicon is smaller than that of crystalline silicon at temperatures below 800 K but greater above 800 K.

## 1 Introduction

Silicon is a very important material in the current electronics industry; for example, single crystalline silicon is commonly used as substrates for large-scale-integrated-circuit (LSI) devices, and amorphous silicon as materials for solar cells. To further improve the productivity of LSI devices, it is essential to produce single crystalline silicon with higher quality as well as larger diameter, for which stricter process design and control should be carried out based upon mathematical modelling for the heat and fluid flow in the crystal growth process. The modelling requires thermophysical property data, including density and heat capacity, for crystalline and liquid silicon with high accuracy, and thus this paper focuses on the density and molar heat capacity at constant pressure of silicon.

Several data have been reported for the density (Grazov *et al* 1969, Sasaki *et al* 1994, Ohsaka *et al* 1997, Rhim and Ohsaka 2000, Paradis *et al* 2003) and molar heat capacity at constant pressure (Serebrennikov and Gel'd 1952, Olette 1957, Kantor *et al* 1960, Barin 1989, Yamaguchi and Itagaki 2002) of silicon; however, there are uncertain factors still remaining in these data. With respect to the density of liquid silicon, there are considerable discrepancies in the temperature coefficients as well as in the absolute values: the temperature

coefficient is negative in any of the above reports but the temperature dependencies reported by Grazov *et al* (1969) and Sasaki *et al* (1994) are stronger than those by the others. There are also considerable discrepancies in published data for the molar heat capacities at constant pressure of solid and liquid silicon; in particular, a big discrepancy can be seen in the change of the heat capacity with melting. Kantor *et al* (1960) and Yamaguchi and Itagaki (2002) have reported that the heat capacity increases discontinuously with melting, whereas the heat capacity recommended by Barin (1989) shows a discontinuous decrease with melting. It is very difficult to understand factors causing such discrepancies but one possibility would be for the contamination of samples by the reaction with sample containers and atmosphere because silicon is chemically active at high temperatures.

Generally, molecular dynamics (MD) simulation would be useful to systems on which it is very difficult to measure. However, it is also difficult to apply MD to silicon due to its complexity of potential because solid silicon is semiconductor but liquid silicon is metallic. Nevertheless, Stillinger and Weber (Stillinger and Weber 1985) have reported a potential of silicon useful for MD simulation, which enables the structure of silicon to be simulated in both crystalline and liquid states. Accordingly, it is likely that thermophysical

properties such as density and heat capacity of silicon can be determined by MD without any effects from chemical contamination. Furthermore, MD can simulate silicon in supercooled liquid and amorphous states and can provide values of the density and heat capacity of silicon in the respective states. In particular, data for amorphous silicon are of scientific interest because bulk amorphous silicon cannot be produced in actuality – amorphous silicon is prepared in the form of thin film most commonly using plasma enhanced chemical vapour deposition. Consequently, the aim of the present work is to determine the density and molar heat capacity at constant pressure of crystalline, liquid and amorphous silicon using MD simulation.

## **2. Simulation condition**

The Stillinger-Weber potential (Stillinger and Weber 1985) was used to express the interaction between silicon atoms - this potential has been constructed so as to reproduce the structures of crystalline silicon and liquid silicon just above the melting point. The unit cell used for MD simulation contained 1000 silicon atoms arranged in the diamond structure, to which cell the three-dimensionally periodic boundary condition was applied. MD simulation was carried out with the aid of the software ‘MASPHYC’ produced

by Fujitsu Co Ltd. The canonical ensemble approach was applied to this simulation, where constant temperature and pressure conditions were established by using the Nosé technique (Nosé 1984, Nosé 1991) and the Parrinello-Rhman technique (Parrinello and Rahman 1981, Ray and Rahman 1984), respectively. Equations of motion for atoms were integrated with a time interval of 1 fs with the use of Gear's fifth-order predictor-corrector algorithm (Berendsen and van Gunsteren 1985).

To obtain the structure of silicon equilibrated at 1 atm and various temperatures, MD simulation was carried out during the heating and cooling cycles using NTP ensemble. First, calculation during the heating cycle was conducted at temperatures between 100 and 2500 K until the system reached equilibrium. The unit cell at the required temperature was constructed on the basis of the structure at a temperature lower than the required temperature, and constant enthalpy for more than 200 ps confirmed that the system was in equilibrium. The volume of the unit cell and the enthalpy and trajectories of atoms at each MD condition were determined from data obtained in the last 20 ps. Second, calculation during the cooling cycle was conducted at temperatures between 3000 – 200 K. For this simulation the unit cell at the required temperature was constructed on the basis of the structure at a temperature higher

than the required temperature, where the initial unit cell was constructed by equilibrating at 4000 K, and constant enthalpy for more than 600 ps confirmed that the system was in equilibrium. The volume of the unit cell and the enthalpy and trajectories of atoms at each MD condition were determined from data obtained in the last 50 ps.

Finally, to determine the density and molar heat capacity at constant pressure with higher accuracy, MD simulation was carried out by means of NVE ensemble using the unit cells obtained in the above. Calculation was conducted for 500 ps at temperatures between 100 and 2500 K and, consequently, mean square displacements of atoms, densities and molar heat capacities at constant pressure were derived from data obtained in the last 50 ps.

### **3. Results and discussion**

Figures 1(a) and 1(b) show the temperature dependencies of (a) volume per unit cell and (b) molar enthalpy for silicon, where the vertical dotted lines represent the experimental melting point of silicon (1683 K). See the changes in the volume per unit cell and the molar enthalpy during the heating cycle. The volume of silicon per unit cell increases monotonically with increasing temperature up to 2300 K and then shows a discontinuous decrease at 2350 K,

followed by another linear increase. The molar enthalpy also increases roughly linearly with increasing temperature up to 2300 K and then shows a discontinuous increase at 2350 K, followed by another linear increase. In addition, the trajectory of silicon atoms showed that atoms moved around lattice sites at temperatures lower than 2300 K, whereas atoms diffused away from lattice sites at 2350 K. From these facts, in this simulation silicon is in solid state at 2300 K and in liquid state at 2350 K and, thus, the melting point of silicon can be estimated in between these temperatures. The melting point estimated is higher than the experimental melting point of silicon (1683 K): this difference is often observed in MD simulation (Kojima and Susa 2002), which would be because silicon in the simulation has no surfaces serving as nucleation sites of melting. From the above facts, the volume per unit cell and the molar enthalpy recorded below 1683 K and above 2350 K correspond to those for crystalline and liquid silicon, respectively.

See the changes in the volume per unit cell and the molar enthalpy during the cooling cycle. The volume per unit cell decreases monotonically with decreasing temperature down to about 1400 K and then shows a steep increase at temperatures between 1400 and 1000 K, followed by a roughly linear decrease.

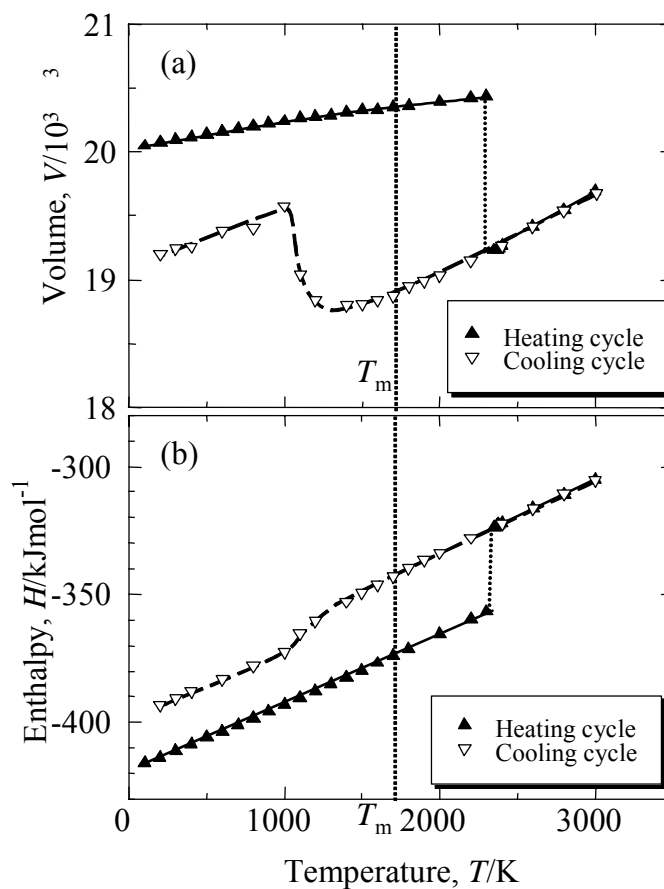


Figure 1 Temperature dependencies of (a) volume per unit cell and (b) molar enthalpy of silicon calculated during heating and cooling cycles.

At temperatures below 2300 K the volume per unit cell recorded during the cooling cycle is smaller than that during the heating cycle. The molar enthalpy decreases linearly with decreasing temperature down to about 1400 K and then shows a steeper decrease at temperatures between 1400 and 1000 K, followed by another linear decrease. The molar enthalpy recorded during the cooling cycle is greater than that during the heating cycle. On the other hand, Figure 2 shows

the change with time in mean square displacements of silicon atoms obtained during the cooling cycle. Mean square displacements of atoms considerably increase with time at temperatures above 1100 K. In addition, the trajectory of atoms at temperatures between 1000 and 300 K during the cooling cycle showed that atoms vibrated near randomly distributing sites. These facts suggest that silicon in the simulation is liquid at temperatures above 1100 K and amorphous below 1000 K. Since the actual melting point of silicon is 1683 K, accordingly, the volume per unit cell and the molar enthalpy recorded above 1100 K and below 1000 K correspond to those for liquid, including supercooled

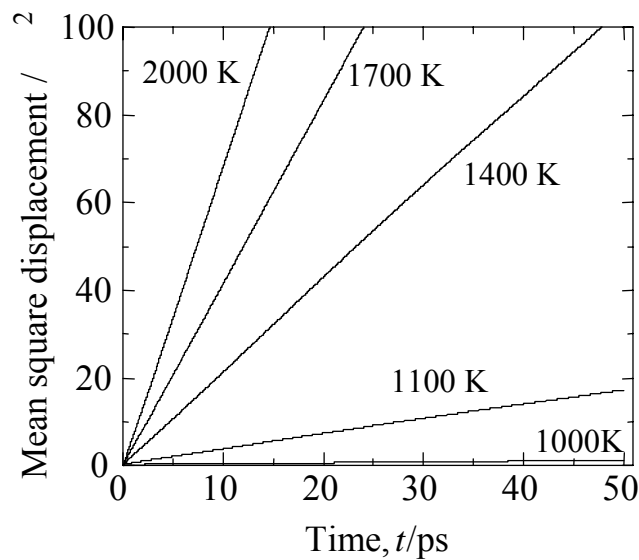


Figure 2 Change with in mean square displacements of silicon atoms during cooling cycle.

liquid, and amorphous silicon, respectively. The latent heat of melting can be estimated from the difference in the enthalpies between solid and liquid silicon at the melting point, leading to  $31.29 \text{ kJmol}^{-1}$ , which is smaller by about 35 % than an experimental value of  $48.31 \text{ kJmol}^{-1}$  reported by Yamaguchi and Itagaki (2002).

Figure 3 shows the densities ( $\rho$ ) of crystalline silicon and liquid silicon including supercooled liquid state as functions of temperature, in comparison

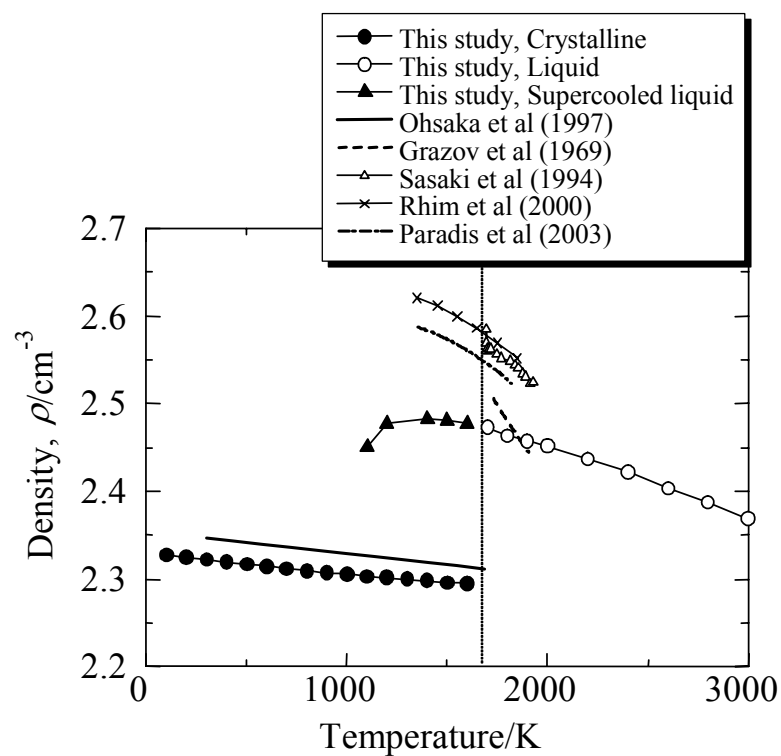


Figure 3 Temperature dependencies of densities of silicon in crystalline, liquid and supercooled states.

with published values (Grazov *et al* 1969, Ohsaka *et al* 1997, Rhim and Ohsaka 2000, Sasaki *et al*, 2002, Paradis *et al* 2003), where density has been calculated from the data in Figure 1(a). The present data indicate that the density of crystalline silicon decreases with increasing temperature and then shows a discontinuous increase at the melting point; in addition, the density of liquid silicon also decreases with temperature. The density of crystalline silicon in the present work is in agreement with those reported by Ohsaka *et al* (1997) with discrepancy less than 1.5 % at temperatures up to the melting point. With respect to the density of liquid silicon, including its supercooled state, the present data are smaller by about 4-5 % than previously reported values. The temperature coefficient of the present data is closer to those recorded by Rhim and Ohsaka (2000) and Paradis *et al* (2003), who measured using the levitation technique, which enables the contamination from sample containers to be eliminated.

Figure 4 summarises the densities of crystalline, liquid and amorphous silicon obtained in the present work. It can be seen that the temperature coefficients of the densities for amorphous and liquid silicon are close to each other although the density of amorphous silicon is smaller than that of the other. Furthermore,

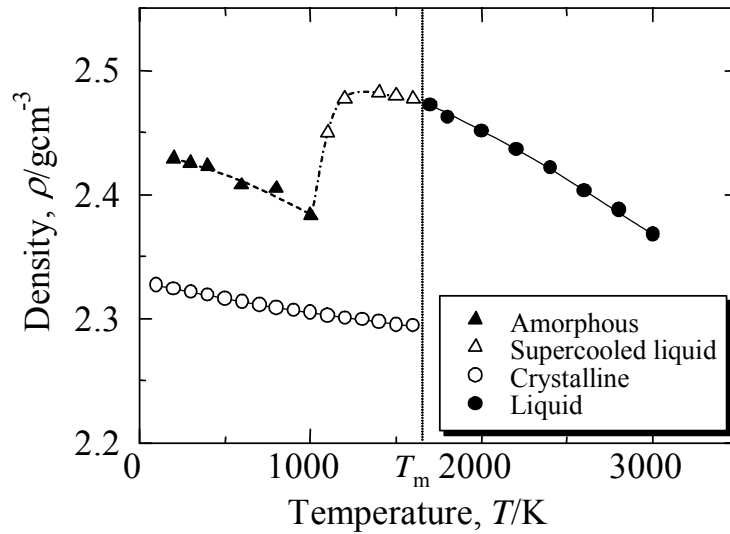


Figure 4 Temperature dependences of densities for silicon in amorphous and supercooled states in comparison with those for crystalline and liquid silicon.

the density of amorphous silicon is greater by about 4 % than that of crystalline silicon; in contrast, there is also a previous study reporting the opposite behaviour (Wood and Young 1984). However, there is a possibility that samples used in the previous study contained a large concentration of impurities such as hydrogen because the samples were prepared using plasma enhanced chemical vapour deposition. Furthermore, the structure of amorphous silicon is close to that of liquid silicon. Accordingly, it is likely that the density of amorphous silicon is greater than that of crystalline silicon. The densities of crystalline, liquid and amorphous silicon can be approximated to the following respective

equations:

Crystalline:

$$\rho = 2.33 - 2.19 \times 10^{-5}T \quad (100 - 1700 \text{ K}) \quad (1)$$

Liquid:

$$\rho = 2.54 - 2.19 \times 10^{-5}T - 1.21 \times 10^{-8}T^2 \quad (1700 - 3000 \text{ K}) \quad (2)$$

Amorphous:

$$\rho = 2.44 - 5.44 \times 10^{-5}T \quad (200 - 1000 \text{ K}) \quad (3)$$

where the units of  $\rho$  is  $\text{gcm}^{-3}$ .

Figure 5 shows the molar heat capacities at constant pressure ( $C_p$ ) for crystalline and liquid silicon as functions of temperature, in comparison with published values (Serebrennikov and Gel'd 1952, Olette 1957, Kantor *et al* 1960, Barin 1989, Yamaguchi and Itagaki 2002). In the present work the heat capacities have been calculated as the derivative of the molar enthalpy in Figure 1(b) with respect to temperature. The heat capacity of crystalline silicon in the present work increases linearly with temperature and then shows a discontinuous increase at the melting point; in contrast, the heat capacity of liquid silicon is a constant value of about  $29 \text{ JK}^{-1}\text{mol}^{-1}$ . On the contrary, Olette (1957) and Barin (1989) have reported that the heat capacity decreases with melting. The present data support the direction of the change reported by Kantor

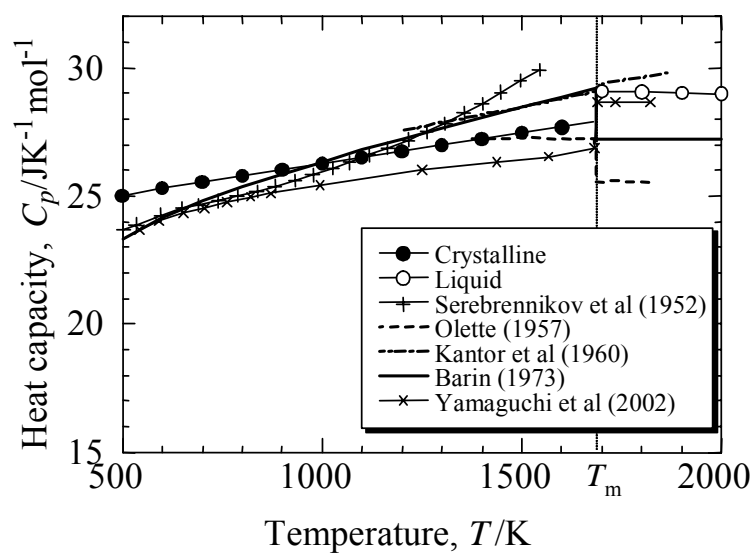


Figure 5 Molar heat capacity at constant pressure for silicon in crystalline and liquid states.

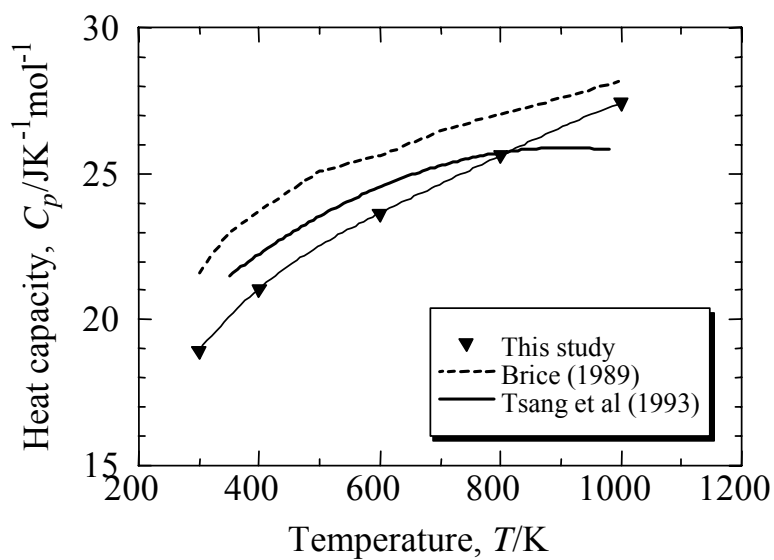


Figure 6 Temperature dependence of molar heat capacity at constant pressure for amorphous silicon.

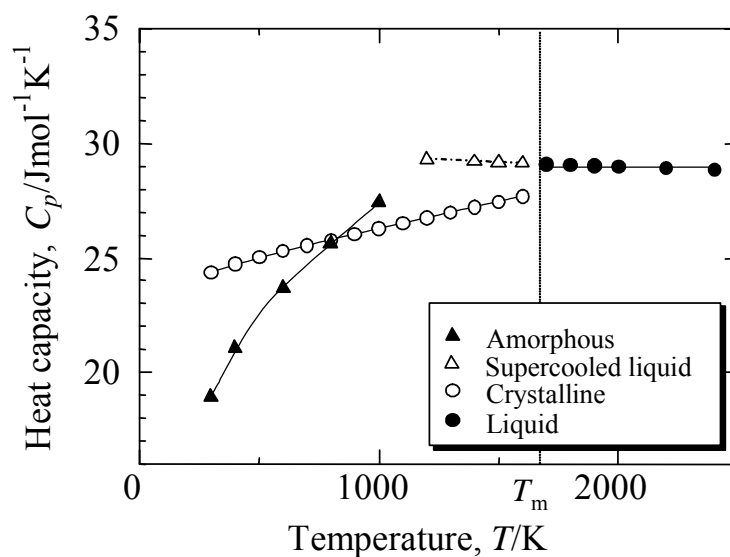


Figure 7 Temperature dependencies of molar heat capacities at constant pressure for amorphous, supercooled, crystalline and liquid silicon.

*et al* (1960) and Yamaguchi and Itagaki (2002) and are on the whole in agreement with values recorded by Yamaguchi and Itagaki (2002).

Figure 6 shows the temperature dependence of the molar heat capacity at constant pressure for amorphous silicon. This figure also includes values reported by Brice (1989) and Tsang *et al* (1993): the former estimated  $C_p$  from both values of the specific heat at constant pressure for crystalline silicon and of the specific heat at constant volume for amorphous silicon, and the latter measured  $C_p$  on amorphous silicon having 20  $\mu\text{m}$  thickness prepared by electron

beam evaporation using a differential scanning calorimeter. The present heat capacity values are in reasonable agreement with the reported values. Figure 7 summarises the molar heat capacities at constant pressure for crystalline, liquid and amorphous silicon obtained in the present work. The heat capacity of amorphous silicon is smaller than that of crystalline silicon at temperatures below 800 K but greater above 800 K. The heat capacities of crystalline, liquid and amorphous silicon can be approximated to the following respective equations:

Crystalline:

$$C_p = 23.5 + 3.05 \times 10^{-3}T - 2.93 \times 10^{-7}T^2 \quad (300 - 1700 \text{ K}) \quad (4)$$

Liquid:

$$C_p = 29.0 \quad (1700 - 2500 \text{ K}) \quad (5)$$

Amorphous:

$$C_p = 13.1 + 2.25 \times 10^{-2}T - 8.30 \times 10^{-6}T^2 \quad (300 - 1000 \text{ K}) \quad (6)$$

where unit of  $C_p$  is in  $\text{J K}^{-1}\text{mol}^{-1}$ .

## Conclusions

The density and molar heat capacity at constant pressure of silicon have been determined with use of molecular dynamics simulation at temperatures between

100 and 2500 K. The density and heat capacity of crystalline, liquid and amorphous silicon can be expressed by Equations 1-3 and Equations 4-6, respectively. The density of amorphous silicon is greater than that of crystalline silicon at temperatures below 1000 K and the heat capacity of amorphous silicon is smaller than that of crystalline silicon at temperatures below 800 K but greater above 800 K.

## References

- Barin I, 1995 *Thermochemical Data of Pure Substances* 3rd ed (New York, VCH)
- Berendsen H J C, van Gunsteren W F, 1985 *Proceeding of the Enrico Fermi Summer School*, Varenna (Bologna: Soc. Italiana de Fisica) pp 43-65
- Brice J C, 1989 *Properties of Amorphous Silicon*, 2<sup>nd</sup> ed, Ed. Fritzsche (INSPED, London) pp 480-482
- Grazov V M, Chizhevskaya S N, Glagoleva N N, 1969 *Liquid Semiconductors*, (New York: Plenum Press) p 61
- Kantor P B, Kisel A N, Fomichev E N, 1960 *Ukr. Fiz. Zh.* **5** 358-362
- Kojima R, Susa M, 2002 *High Temperatures-High Pressures*, **34** 639-648
- Nosé S, 1984 *Mol. Phys.* **52** 255-268

- Nosé S, 1991 *Progress of Theoretical physics Supplement* **103** 1-46
- Ohsaka K, Chung S K, Rhim W K, 1997 *Appl. Phys. Lett.* **70** 423-425
- Olette M, 1957 *Compt. Rend.* **244** 1033-1036
- Paradis P F, Ishikawa T, Yoda S, 2003 *J. JPN. Soc. Microgravity Appl.* **20**  
218-225
- Parrinello M, Rahman A, 1981 *J. Appl. Phys.* **52** 7182-7190
- Ray J R, Rahman A, 1984 *J. Chem. Phys.* **80** 4423-4428
- Rhim W -K, Ohsaka K, 2000 *J Crystal Growth* **208** 313-321
- Sasaki H, Tokizaki E, Terashima K, Kimura S, 1994 *Jpn. J. Appl. Phys.* **33**  
3803-3807
- Serebrennikov N M, Gel'd P V, 1952 *Dokl. Akad. Nauk SSSR* **87** 1021
- Stillinger F H, Weber T A, 1985 *Phys. Rev. B* **31** 5262-5271
- Tsang K H, Kui H W, Chik K P, 1993 *J. Appl. Phys.* **74** 4932-4935
- Wood R F, Young R T, 1984 *Pulsed Laser Processing of Semiconductors*, vol.  
23 of *Semiconductors and Semimetals* (Academic, New York) p 191
- Yamaguchi K, Itagaki K, 2002 *J. Thermal Analysis and Calorimetry* **69**  
1059-1066